Supporting Information

# Phosphate Ester-based Organocatalyst with Strong Electron-withdrawing Substituents for Efficient Chemical Recycling of Poly(lactic acid)

Huajuan Zhai, Yujie Fang, Sihuai Fan, Wanhua Wu, Tao Sun, Weihan Rao, Jiandong Ding and Lin Yu*

**Table of Contents**

## 1. Materials

*p*-Cresol, *p*-methoxyphenol, *p*-trifluoromethylphenol, *p*-fluorophenol, *m*-nitrophenol, $POCl_3$, lactic acid solution (85%), DPP, $Sn(Oct)_2$, triethylamine (TEA), ZnO, lithium chloride (LiCl), aluminum chloride ($AlCl_3$), calcium oxide (CaO), *p*-TsOH, anhydrous toluene and anhydrous acetonitrile were supplied by Adamas Reagent, Ltd. (China). *o*-Nitrophenol and *p*-nitrophenol were bought from Tokyo Chemical Industry Co., Ltd. (Japan). The pharmaceutical secondary standard lactic acid was obtained from Supelco of the Merck Group. PLA pellets such as Luminy® LX175, Luminy® L105 and Luminy® LX530 were acquired from TotalEnergies Corbion, while Ingeo™ 6060D, Ingeo™ 4032D, Ingeo™ 3260HP were supplied by NatureWorks LLC. PLA products, including 3D printing materials, cups, shopping bags, unwoven fabric, masks, and yarn, as well as durable plastics such as LDPE, HDPE, PET, PP, PS, and PVC were purchased as commercial products from the Taobao website and used without further purification. PLA trimmings were bought from Dongguan Xinyue Cai Plastic Co., Ltd. (China). PBAT (ecoflex® F Blend C1200) was sourced from BASF SE; PBS (BioPBSTM FD72PM) was provided by Mitsubishi Corporation; PBSA (5001MD) was obtained from Showa Denko K.K.; PTMC was supplied from Daigang Biological Technology CO., Ltd. (China); PHB (P209) was sourced from BiomeR GmbH; PCL (CAPA® 6800) was purchased from Perstorp. Other reagents were the products of Sinopharm Chemical Reagent Co. (China). Dichloromethane (DCM) was dried with calcium hydride and re-distilled before each use. Unless otherwise specified, all other reagents were used as received without further purification.

## 2. Experimental Procedures

### 2.1 Characterization and Experimental Setup

#### NMR Detection

Samples were dissolved in 600 μL of $CDCl_3$ or DMSO-$d_6$ based on their respective solubility. Subsequently, $^1$H NMR, $^{31}$P NMR and $^{13}$C NMR spectra were recorded using a 400 MHz NMR spectrometer (Bruker, AVANCE III HD) at 25 °C.

#### GPC Analysis

Samples, dissolved in THF or $CHCl_3$ based on their respective solubility, were analyzed at 35 °C with a flow rate of 1.0 mL/min using THF or $CHCl_3$ as the eluent in a GPC system (Agilent, 1260). Narrowly distributed PS was employed as the calibration standard. The $M_n$s and $Đ_M$ values of various polymer samples before and after degradation were confirmed.

#### HRMS Analysis

The MWs of the synthesized DPP derivatives were determined using a high solution mass spectrometer (Waters, G2-xs tof) equipped with an electrospray ionization (ESI) source. The experimental parameters were configured as follows: capillary voltage set to 2.4 kV, sampling cone voltage adjusted to 30 V, source temperature maintained at 130 °C, and desolvation temperature set to 500 °C.

#### MALDI-TOF MS Measurement

The MALDI-TOF mass spectrum of OLA was obtained via a MALDI-TOF/TOF mass spectrometer (AB SCIEX, 5800) equipped with a neodymium-doped yttrium aluminum garnet laser (ND-YAG, 355 nm wavelength, 400 Hz). OLA was mixed with trans-2-[3-(4-tert-butylphenyl)-2-methyl-2-propenylidene] malononitrile (DCTB) as the matrix and sodium trifluoroacetate as the ionization agent, and then dissolved in THF. 0.5 μL of sample was dropped onto the sample plate. Once the solvent had completely evaporated, the plate was placed into the instrument for analysis. The measurement was carried out in reflection mode using the positive ionization method.

#### HPLC Measurement

The mass fraction of lactic acid in the degradation products was determined using an HPLC system (Waters, e2695) equipped with a C18 reversed-phase column (XBridge™ BEH130, 4.6 × 250 mm, 5 mm) and a UV detector (Waters, 2489). The experiment was carried out with the injection volume of 20 μL at a flow rate of 1 mL/min. The UV absorption was measured at 210 nm, and the analysis was conducted at 40 °C using a mixture of 97 vol% water (containing 1% phosphoric acid) and 3 vol% acetonitrile as the eluent.

#### ATR-FTIR Spectroscopy Analysis

The durable plastic fragments before and after treatment were analyzed on an infrared spectrometer (ThermoFisher, Nicolet 6700) installed with an attenuated total reflectance accessory (PIKE Gladi-ATR). After measuring the blank background spectrum, the samples were placed in the testing area and pressed tightly to obtain the spectra in the 400-4000 $cm^{-1}$ band.

**DSC Analysis**

A differential scanning calorimeter (TA, DSC250) was employed to assess the thermal properties of samples. About 5 mg of each sample was placed in an aluminum pan and sealed. The tests were carried out under a nitrogen atmosphere with a flow of 50 mL/min. For LA monomer, the sample was heated to 140 °C at a rate of 10 °C/min. For repolymerized PLA, the sample was heated to 200 °C at the same rate, held for 5 min to erase any thermal history, and then cooled to 20 °C at 10 °C/min. After equilibrating for 5 min, the samples were reheated to 200 °C at 10 °C/min, and the data of reheating process were recorded. To measure the $X_c$ of various PLA pellets, the final heating rate was reduced to 5 °C/min. The crystallinity ($X_c$) data were calculated via the following formula:

$$X_{\mathrm{c}}\ (\%) = \frac{\Delta H_{\mathrm{f}} - \Delta H_{\mathrm{cc}}}{\Delta H_{\mathrm{f}}^{0}} \times 100\% \tag{S1}$$

where $\Delta H_{\mathrm{f}}$ and $\Delta H_{\mathrm{cc}}$ represent the measured melting enthalpy and cold crystallization enthalpy, respectively. $\Delta H_{\mathrm{f}}^{0}$ indicates the melting enthalpy of completely crystalline PLA, which is 93 J/g.[1]

**TGA Analysis**

The thermal stability of durable plastic fragments before and after treatment was analyzed using a thermogravimetric analyzer (Mettler, TGA 1) under a nitrogen atmosphere with a flow rate of 50 mL/min. A sample of 5-15 mg was weighed in a ceramic crucible and positioned inside the furnace. After background subtraction, the temperature was increased to 80 °C at the rate of 10 °C/min, held for 5 min to remove trace water, and then further increased to 600 °C at the same heating rate.

**Specific Rotation Measurement**

The specific rotations of LA and PLA in chloroform solutions, and calcium lactate in aqueous solution were determined using an automatic polarimeter (Autopol VI, Rudolph Research Analytical) at 25 °C with a wavelength of 589 nm. The L-configuration ratios of samples were calculated via the following formula:

$$\text{L ratio}\ (\%) = \frac{[\alpha_0]_{\mathrm{D}}^{25} + [\alpha]_{\mathrm{D}}^{25}}{2[\alpha_0]_{\mathrm{D}}^{25}} \times 100\% \tag{S2}$$

where $[\alpha]_{\mathrm{D}}^{25}$ represents the measured specific rotation, and $[\alpha_0]_{\mathrm{D}}^{25}$ refers to the specific rotation of the corresponding optically pure substance. The specific rotation of PLLA was determined based on measurements conducted on L105 PLA pellets (L-isomer content% > 99 %).

**Assessment of Green Chemistry Metrics**

The energy economy coefficient ($\varepsilon$), environmental factor (*E* factor) and environmental energy impact factor ($\xi$ factor) were calculated as follows:[2]

$$\varepsilon = \frac{Y}{T \times t} \tag{S3}$$

$$E\ \text{factor} = \frac{\text{mass of waste}}{\text{mass of product}} = \frac{[0.1 \times \text{solvent ratio} + \text{catalyst ratio}] \times m_{\mathrm{PLA}}}{Y \times \frac{M_{\mathrm{product}}}{M_{\mathrm{PLA\ units}}} \times m_{\mathrm{PLA}}} \tag{S4}$$

$$\xi\ \text{factor} = \frac{E\ \text{factor}}{\varepsilon} \tag{S5}$$

where *Y*, *T* and *t* denote the product yield, temperature (in degrees celsius) and time (in minutes), respectively. $M_{\mathrm{product}}$ and $M_{\mathrm{PLA\ units}}$ represent the molar mass of the product and its corresponding repeating units. For the solvent ratio, a correction factor of 0.1 was introduced, assuming a 90% recycling rate in industry.[2]

**2.2 Synthesis of DPP Derivatives**

**Synthesis of *p*-Bis-methylphenyl Phosphate**

The synthesis of *p*-bis-methylphenyl phosphate was conducted according to the procedure described in previous research.[3] Specially, anhydrous toluene (30 mL), *p*-cresol (11.35 g, 0.105mol), and aluminum chloride (0.280 g, 0.002mol) were added into a flask under an argon atmosphere. Subsequently, TEA (14 mL, 0.1 mol) and $POCl_3$ (4.7 mL, 0.05 mol) were introduced into the reaction system. The solution was stirred at room temperature for 0.5 h, followed by heating to 90 °C and refluxing for 3 h. After the reaction was completed, 10 mL of water was added and the mixture was stirred at room temperature for 10 min. The organic phase was separated, concentrated, and then refluxed in a mixture of 50 mL acetone and 5 mL water for 1 h. Following this, the reaction system was extracted with 1 M $Na_2CO_3$ solution. The collected aqueous phase was washed three times with DCM, treated with dilute hydrochloric acid and then exacted with DCM. Finally, the collected organic phase was evaporated under reduced pressure to yield a white solid (5.76 g, yield: 41.4%).

Spectra for the product: $^1$H NMR (400 MHz, $CDCl_3$): $\delta$ 7.06-6.97 (m, 8H), 2.27 (s, 6H); $^{13}$C NMR (100 MHz, $CDCl_3$): $\delta$ 148.82 (d, $J$ = 7.3 Hz), 134.13, 129.97, 119.94 (d, $J$ = 4.8 Hz), 20.68; $^{31}$P NMR (161 MHz, $CDCl_3$): $\delta$ -9.86; HRMS (ESI): *m/z* calcd. for C14H16O4P: 279.0786 $[M+H]^+$; found 279.0786.

**Synthesis of *p*-BMOPP**

*p*-BMOPP was synthesized according to previous research.[4] Specifically, *p*-methoxyphenol (2.38 g, 0.019 mol), $POCl_3$ (2.89 g, 0.019mol) and LiCl were heated in a Schlenk tube under an argon atmosphere at 110 °C for 24 h. Then, 10 mL of water was added, and the reaction mixture was heated under 90 °C for 16 h. Upon completion of the reaction, the system was dissolved in 50 mL DCM and subsequently extracted with 20 mL of 1 M $Na_2CO_3$ solution. The collected aqueous phase was washed three times with 10 mL of DCM, and then acidified with 1 M HCl. The product was then extracted from the aqueous phase using DCM. Finally, the collected organic phase was steamed under reduced pressure to obtain a white solid (1.72 g, yield: 58.3%).

Spectra for the product: $^1$H NMR (400 MHz, $CDCl_3$): $\delta$ 7.08 (d, $J$ = 9.6 Hz, 4H), 6.80 (d, $J$ = 8.8 Hz, 4H), 3.77 (s, 6H); $^{13}$C NMR (100 MHz, $CDCl_3$): $\delta$ 156.86, 144.02 (d, $J$ = 7.0 Hz), 121.09 (d, $J$ = 4.6 Hz), 114.59, 55.56; $^{31}$P NMR (161 MHz, $CDCl_3$): $\delta$ -8.87; HRMS (ESI): *m/z* calcd. for C14H16O6P: 311.0684 $[M+H]^+$; found: 311.0685.

**Synthesis of *p*-Bis-trifluoromethylphenyl Phosphate**

The synthesis procedure for *p*-bis-trifluoromethylphenyl phosphate was identical to that of *p*-BMOPP. A white solid was obtained with a yield of 9.8%.

Spectra for the product: $^1$H NMR (400 MHz, DMSO-$d_6$): $\delta$ 7.64 (d, $J$ = 8.6 Hz, 4H), 7.35 (d, $J$ = 8.4 Hz, 4H); $^{13}$C NMR (100 MHz, DMSO-$d_6$): $\delta$ 155.29 (d, $J$ = 6.8 Hz), 127.47 (q, $J$ = 3.9 Hz), 124.81 (q, $J$ = 32.3 Hz), 124.65 (q, $J$ = 270.0 Hz), 121.00 (d, $J$ = 5.2 Hz); $^{31}$P NMR (161 MHz, DMSO-$d_6$): $\delta$ -12.73; HRMS (ESI): *m/z* calcd. for C14H8F6O4P: 385.0064 $[M-H]^-$; found 385.0064.

**Synthesis of p-Bis-fluorophenyl Phosphate**

The synthesis procedure for *p*-bis-fluorophenyl phosphate was also identical to that of *p*-BMOPP. A white solid was obtained with a yield of 10.0%.

Spectra for the product: $^1$H NMR (400 MHz, $CDCl_3$): $\delta$ 7.16-7.07 (m, 4H), 6.99 (t, $J$ = 8.5 Hz, 4H); $^{13}$C NMR (100 MHz, $CDCl_3$): $\delta$ 159.95 (d, $J$ = 244.2 Hz), 146.07, 121.57 (dd, $J$ = 8.5, 4.7 Hz), 116.39 (d, $J$ = 23.5 Hz); $^{31}$P NMR (161 MHz, $CDCl_3$): $\delta$ -10.21; HRMS (ESI): *m/z* calcd. for C12H8F2O4P: 285.0128 $[M-H]^-$; found: 285.0128.

**Synthesis of *p*-BNPP**

*p*-BNPP was synthesized according to the procedure described in previous studies.[5,6] In brief, *p*-nitrophenol (3.48 g, 0.025 mol) was added in a Schlenk flask, and the atmosphere was replaced with argon for three times. Anhydrous acetonitrile was then injected to dissolve the mixture. In an ice-water bath, TEA (3.48 mL, 0.025 mol) was added, followed by the addition of $POCl_3$ (1.28 mL, 0.014 mol) diluted with acetonitrile. The reaction was allowed to proceed at room temperature for 24 h.

Upon completion, the reaction solution was slowly dropped into cold water to induce precipitation. The white solid, *p*-TNPP, was collected by filtration.

The obtained *p*-TNPP (3.0 g, 0.007 mol) was dissolved in a mixed solvent of acetonitrile and water. 4 M NaOH solution (8 mL) was added, and the mixture was stirred for 30 min. The solution was then neutralized to pH = 4 using IR-120 ($H^+$) resin. The resin was filtered off, and the filtrate was collected and concentrated via rotary evaporation to remove acetonitrile. The concentrated aqueous phase was repeatedly exacted with ether until the extracted ether no longer turned yellow upon contact with aqueous alkali. Upon acidification of the collected aqueous phase with dilute hydrochloric acid, *p*-BNPP was precipitated and collected by filtration (0.56 g, yield: 13.2 %). Finally, *p*-BNPP was purified by recrystallization in deionized water.

Spectra for the product: $^1$H NMR (400 MHz, DMSO-$d_6$): $\delta$ 8.22 (d, $J$ = 9.2 Hz, 4H), 7.40 (d, $J$ = 9.2 Hz, 4H); $^{13}$C NMR (100 MHz, DMSO-$d_6$): $\delta$ 158.48 (d, $J$ = 6.4 Hz), 143.14, 125.97, 120.86 (d, $J$ = 5.3 Hz); $^{31}$P NMR (161 MHz, DMSO-$d_6$): $\delta$ -13.48; HRMS (ESI): *m/z* calcd. for C12H8N2O8P [M-H]$^-$: 339.0018; found 339.0018.

**Synthesis of *o*-BNPP**

The synthesis procedure for *o*-BNPP was also identical to that of *p*-BNPP. A white solid was obtained with a yield of 29.9%.

Spectra for the product: $^1$H NMR (400 MHz, DMSO-$d_6$): $\delta$ 7.95-7.75 (m, 2H), 7.68-7.50 (m, 4H), 7.30-7.20 (m, 2H); $^{13}$C NMR (100 MHz, DMSO-$d_6$): $\delta$ 145.60 (d, $J$ = 6.3 Hz), 142.13 (d, $J$ = 6.8 Hz), 134.22, 125.06, 123.82, 122.71 (d, $J$ = 2.8 Hz); $^{31}$P NMR (161 MHz, DMSO-$d_6$): $\delta$ -13.27; HRMS (ESI): *m/z* calcd. for C12H8N2O8P: 339.0018 [M-H]$^-$; found 339.0018.

**Synthesis of *m*-BNPP**

The synthesis procedure for *m*-BNPP was also identical to that of *p*-BNPP. Upon acidification, the resulting solution was lyophilized, and subsequently recrystallized from a 1:1 (v/v) mixture of acetone and petroleum ether, yielding a white solid with a yield of 47.0%.

Spectra for the product: $^1$H NMR (400 MHz, DMSO-$d_6$): $\delta$ 8.07-8.03 (m, 2H), 8.00-7.94 (m, 2H), 7.65-7.57 (m, 4H); $^{13}$C NMR (100 MHz, DMSO-$d_6$): $\delta$ 153.27 (d, $J$ = 6.7 Hz), 148.73, 131.22, 127.31 (d, $J$ = 5.8 Hz), 118.79, 115.04 (d, $J$ = 4.6 Hz); $^{31}$P NMR (161 MHz, DMSO-$d_6$): $\delta$ -12.41; HRMS (ESI): *m/z* calcd. for C12H8N2O8P: 339.0018 [M-H]$^-$; found 339.0018.

**2.3 Catalytic Hydrolysis of PLA**

As a typical example, in a 25 mL Schlenk tube equipped with magnetic stirring and a reflux condenser, 1.50 g of LX175 PLA, 0.053 g of *p*-BNPP and 0.45 g of $H_2O$ were added in sequence. The reaction mixture was then placed into a 160 °C oil bath and allowed to react in open air for 30 min. Upon completion, the reaction system was rapidly cooled and sampled. Unless otherwise noted in the Results section regarding any changes to the sample, catalyst, reaction temperature, reaction time, or feeding ratio, the reaction was performed as described above.

The degradation residues were dissolved in 600 μL of DMSO-$d_6$, and 75 μL of $D_2O$ was added to equilibrate the baseline. For samples with high MWs that exhibited low solubility in DMSO-$d_6$, $CDCl_3$ was used as the solvent. The $\overline{\mathrm{DP}}$ of degraded residues was determined by $^1$H NMR analysis, with the specific calculation method described as follows:

$$\overline{\mathrm{DP}} = 1 + \frac{I_{1.46-1.38}}{I_{1.23} + I_{1.27}} \tag{S6}$$

where $I_{1.23}$ represents the integral area of methyl protons in lactic acid (HOCOCH(C***H*****$_3$**)OH), $I_{1.27}$ corresponds to the integral area of terminal methyl protons in OLA (-COCH(C***H*****$_3$**)OH), and $I_{1.46-1.38}$ reflects the integral area of other methyl protons in OLA (-COCH(C***H*****$_3$**)O-).

To measure the conversion, the degradation residues were dissolved in water with sonication for three cycles. The insoluble fractions were then collected, lyophilized and weighed. The conversion was calculated as shown in the following equation:

$$\text{Conversion (\%)} = \left(1 - \frac{m_{\text{residue}}}{m_{\text{total}}}\right) \times 100\% \tag{S7}$$

where $m_{\text{total}}$ represents the mass of initial residues, and $m_{\text{residue}}$ represents the mass of lyophilized residues.

The Hammett equation was utilized for the linear fitting of the PLA hydrolysis reaction mediated by DPP derivatives, with the *x*-axis representing the substituent constant $\sigma_x$ and the *y*-axis indicating the logarithm of the ratio of the reaction rate constants.[7] In the present study, the *y*-axis was simplified as follows:

$$\lg\frac{k_{\mathrm{X}}}{k_{\mathrm{H}}}=\lg\frac{v_{\mathrm{X}}}{v_{\mathrm{H}}}\approx\lg\frac{\left(\overline{\mathrm{DP}_0}-\overline{\mathrm{DP}_{\mathrm{X}}}\right)/t_{\mathrm{X}}}{\left(\overline{\mathrm{DP}_0}-\overline{\mathrm{DP}_{\mathrm{H}}}\right)/t_{\mathrm{H}}} \tag{S8}$$

where $k_{\mathrm{X}}$ and $k_{\mathrm{H}}$represent the rate constants for the hydrolysis of PLA catalyzed by the DPP derivative with substituent X, and DPP, respectively. $v_{\mathrm{X}}$ and $v_{\mathrm{H}}$ denote the reaction rates for the hydrolysis of PLA catalyzed by the DPP derivative with substituent X, and DPP, respectively. $\overline{\mathrm{DP}_0}$, $\overline{\mathrm{DP}_{\mathrm{X}}}$ and $\overline{\mathrm{DP}_{\mathrm{H}}}$ indcate the $\overline{\mathrm{DP}}$ of LX175 PLA, its degradation residues catalyzed by the DPP derivative with substituent X, and DPP, respectively. $t_{\mathrm{X}}$ and $t_{\mathrm{H}}$ mean the respective reaction time.

To investigate the degradation of PLA discs under identical pH conditions, LX175 PLA pellets were dissolved in DCM, cast into a Petri dish, and dried to form a film. PLA discs (8 × 8 mm, 35 ± 5 mg) were then obtained, and each disc was immersed in 2 mL of either $H_2O$ or *p*-BNPP/HCl/*p*-TsOH aqueous solution and incubated at 70 °C. At predetermined intervals, the residues were rinsed with deionized water and methanol, dried, and their residual mass was recorded.

**2.4 Computational Details of DFT Calculations**

All structures and their complexes were subjected to structural optimization at the theoretical level of B3LYP/6-311g (d, p) with PCM solvation model in water, using the Gaussian 9 program.[8] The long range van der Waals interactions were described by the DFT-D3 approach,[9] as this method has great advantages in treating London-dispersion interactions and van der Waals Interactions. The reaction temperature was set to 423.15 K, approaching the conditions conducted in the experiments. All 3D-model graphics were generated using the CYLview program.[10]

**2.5 Synthesis of LA Monomer**

LA was synthesized following the conventional industrial route. In brief, 100 g of OLA was introduced into a 250 mL four-necked flask equipped with a thermometer, mechanical stirrer, and Claisen distillation head. The system was heated to 155 °C under reduced pressure for 0.5 h to remove the residual water in OLA. Under an argon atmosphere, 0.75 g of ZnO was introduced as the catalyst. The reaction was carried out under a pressure of less than 3 kPa and at a temperature of 230 °C. Crude LA was continuously steamed from the reaction system and cooled by a condensing tube with 85 °C hot water as the colling medium (yield: 70.8%). The purified LA, appearing as white needle-like crystals, was obtained by washing with distilled water and recrystallizing three times with ethyl acetate.

**2.6 Repolymerization of PLA**

Repolymerized PLA was obtained via $Sn(Oct)_2$-catalyzed ROP of LA. Briefly, 5 g of purified LA was added into a dry ampoule and degassed at 70 °C to remove residual moisture. Under an argon atmosphere, $Sn(Oct)_2$ (1.5 mg) diluted with anhydrous DCM (0.5 mL) was injected into the ampoule. As the reaction mixture was purged with argon three times and evacuated to approximately 60 Pa, the ampoule was flamed-sealed and immersed in an oil bath at 140 °C for 12 h. Upon completion of the polymerization, the crude products were retrieved by breaking the ampule, dissolved in DCM, and then precipitated in methanol. After drying the precipitation under vacuum for 24 h, the repolymerized PLA was harvested.

**2.7 Synthesis of Calcium Lactate**

4.0 g of CaO, 50 mL of deionized water and 12 mL of commercial L-lactic acid solution or lactic acid solution obtained from the *p*-BNPP-catalyzed hydrolysis of LX175 PLA were added into a flask. The reaction mixture was stirred at room temperature for 70 min, followed by heating to 80 °C. After hot filtration, the filtrate was allowed to crystallize at 4 °C. Subsequently, the solid product was collected via filtration, washed three times with ethanol, and vacuum-dried for 24 h. The resulting powder was further treated at 120 °C to remove any bound water, yielding L-calcium lactate and self-made calcium lactate as a white powder.

**2.8 Scale-up Hydrolysis of PLA**

The scale-up experiment of PLA hydrolysis mediated by *p*-BNPP was conducted in a 5 L reactor. In brief, 1.0 kg of PLA trimmings, 35 g of *p*-BNPP and 83 g of $H_2O$ were added into the reactor, and the mixture was heated at 160 °C for 30 min. Subsequently, an additional 1.0 kg of PLA trimmings along with 83 g of $H_2O$ were promptly introduced, followed by prolonging

the reaction time for another 30 min. The procedure was repeated three times, resulting in the degradation of 4.0 kg of PLA trimmings within 2 h. Upon completion of the reaction, the obtained OLA was collected and analyzed.

Additionally, the collected OLA was further hydrolyzed into a high-concentration lactic acid solution in the reactor. In brief, 1.5 kg of OLA and 0.75 kg of $H_2O$ were added into the reactor, and the mixture were hydrolyzed at 95 °C for 9 h. After that, the product was collected and analyzed.

## 3. Supplementary Results

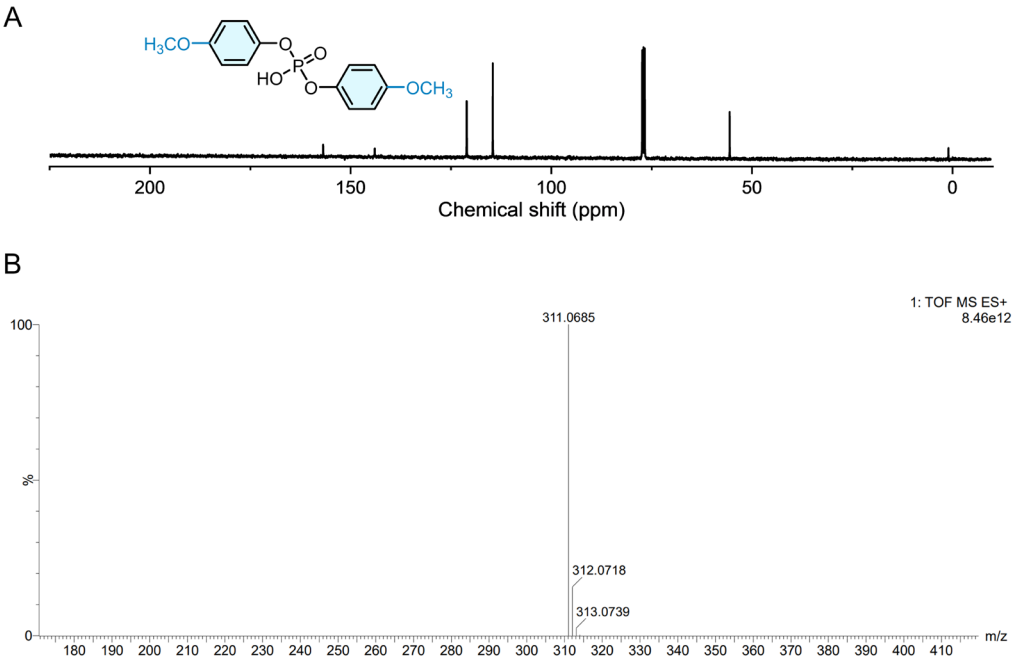


**Fig. S1.** Characterization of *p*-BMOPP. $^{13}C$ NMR (A) and HRMS (B) spectra of *p*-BMOPP.

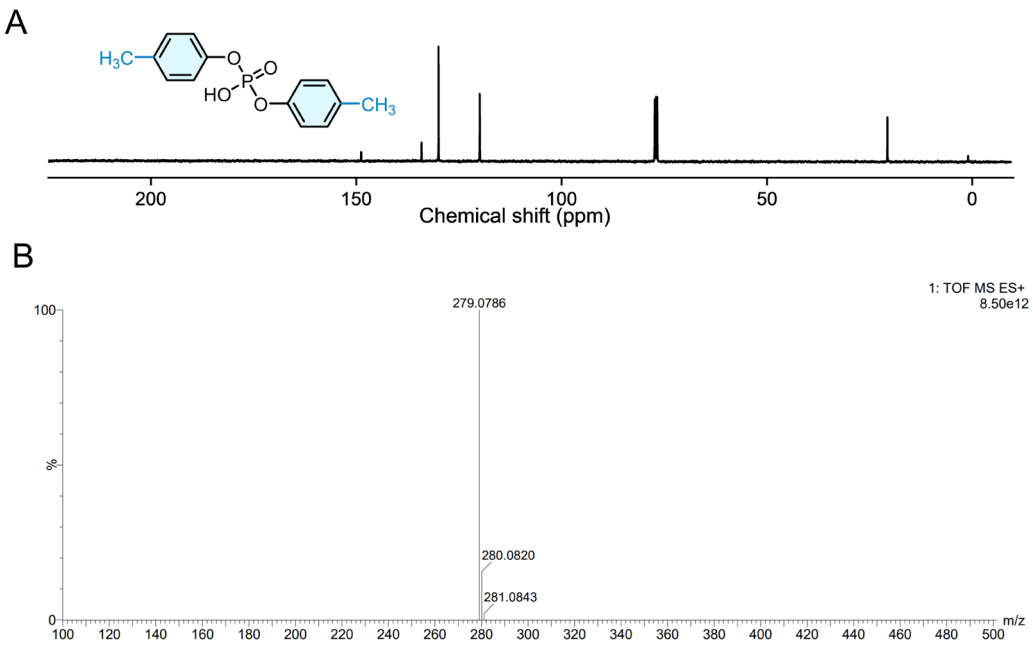


**Fig. S2.** Characterization of *p*-bis-methylphenyl phosphate. $^{13}C$ NMR (A) and HRMS (B) spectra of *p*-bis-methylphenyl phosphate.

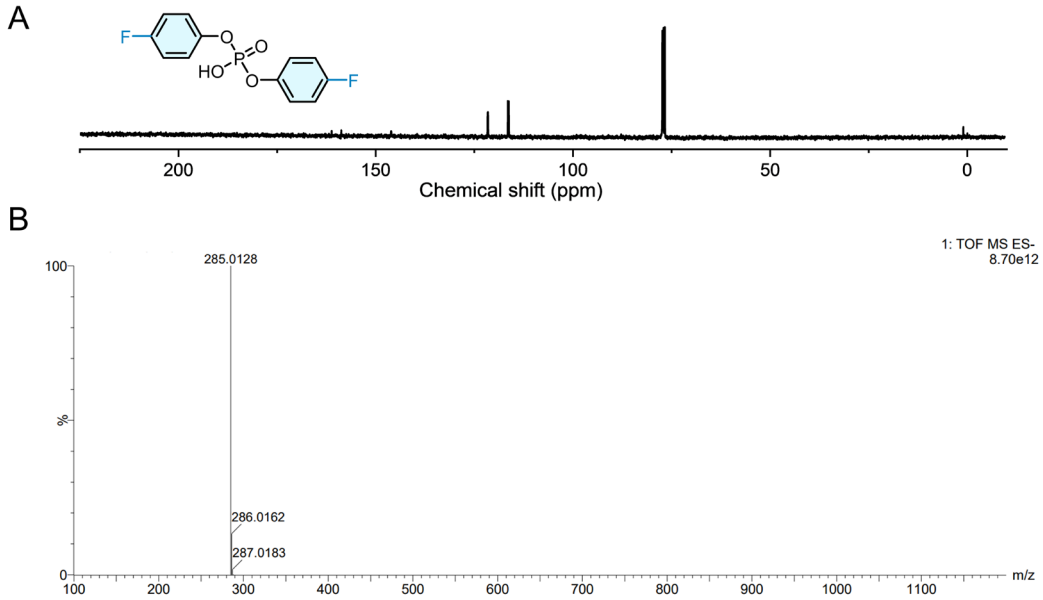


**Fig. S3.** Characterization of *p*-bis-fluorophenyl phosphate. $^{13}C$ NMR (A) and HRMS (B) spectra of *p*-bis-fluorophenyl phosphate.

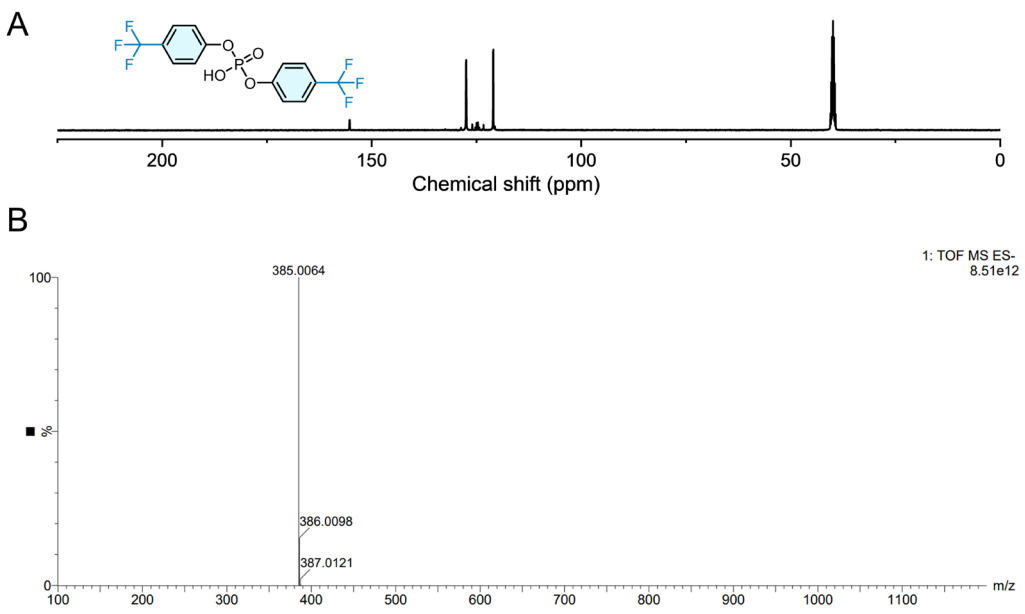


**Fig. S4.** Characterization of *p*-bis-trifluoromethylphenyl phosphate. $^{13}C$ NMR (A) and HRMS (B) spectra of *p*-bis-trifluoromethylphenyl phosphate.

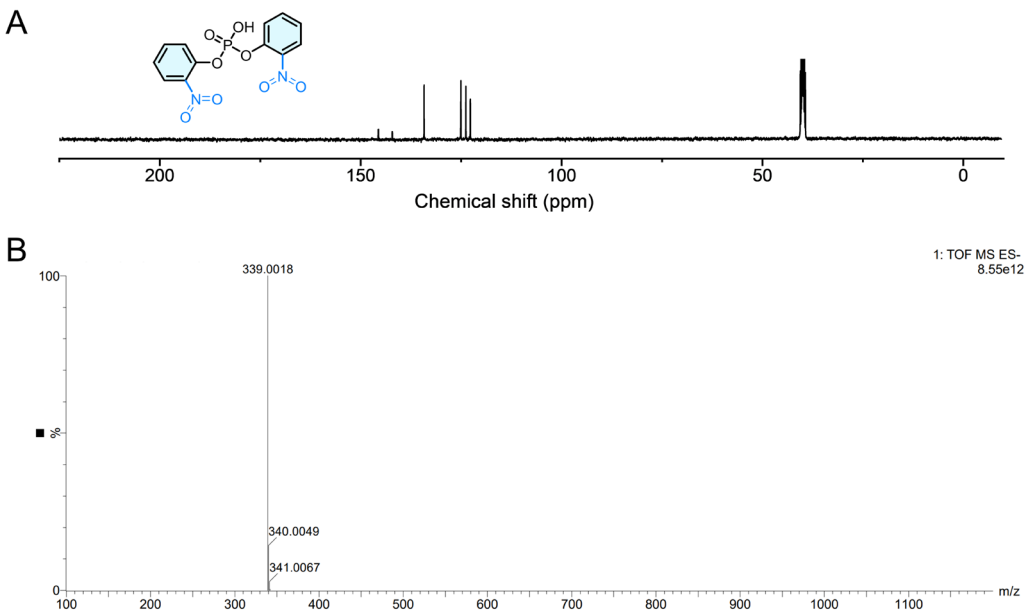


**Fig. S5.** Characterization of *o*-BNPP. $^{13}C$ NMR (A) and HRMS (B) spectra of *o*-BNPP.

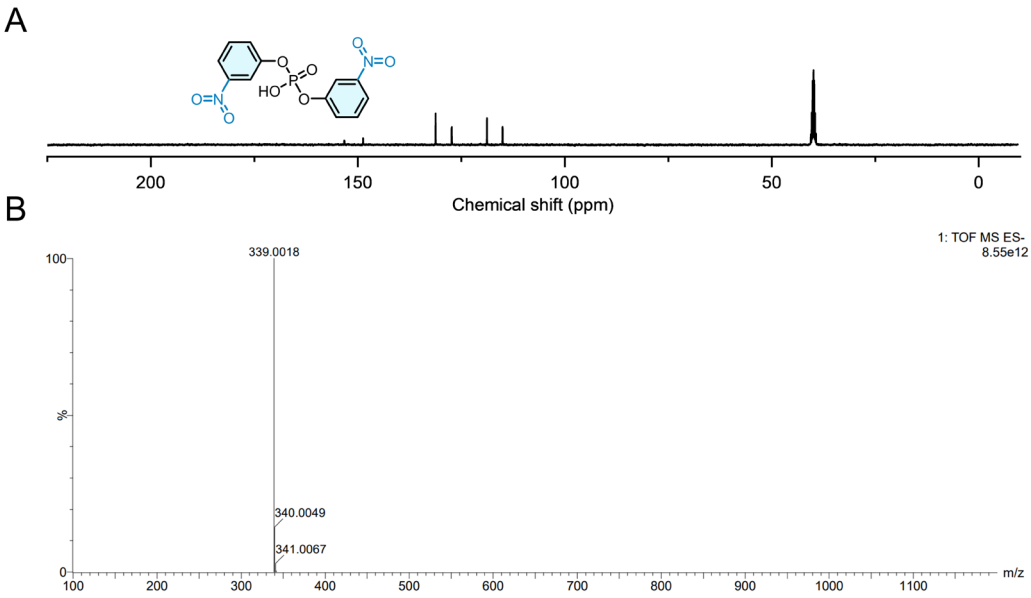


**Fig. S6.** Characterization of *m*-BNPP. $^{13}C$ NMR (A) and HRMS (B) spectra of *m*-BNPP.

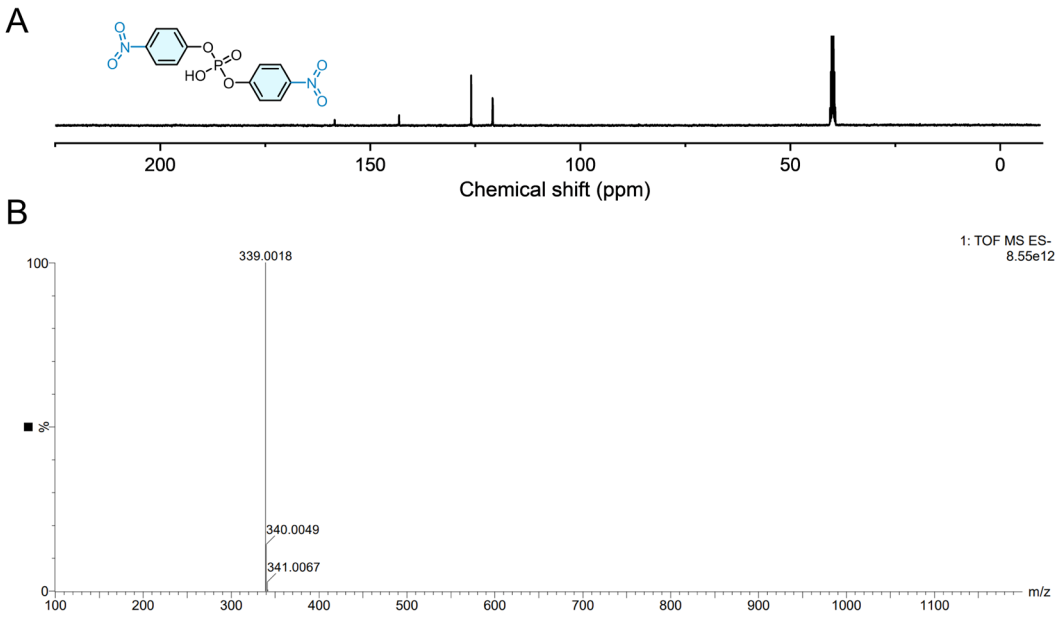


**Fig. S7.** Characterization of *p*-BNPP. $^{13}C$ NMR (A) and HRMS (B) spectra of *p*-BNPP.

**Table S1.** $^{31}P$ NMR chemical shifts of various phenyl phosphate esters reported in previous studies.

| Sample | Substituents on the benzene ring | Chemical shift of $^{31}P$ (ppm) | Solvent | Auxiliary characterization | Ref. |
|---|---|---|---|---|---|
| Monophenyl phosphate esters | -H | -4.8 | $D_2O$ | - | [11] |
| | *p*-$NO_2$ | -4.8 | Water | - | [12] |
| Diphenyl phosphate esters | *p*-$^{t}$Bu | -9.0 | $CDCl_3$ | FTIR; MS | [4] |
| | *p*-$^{n}$Bu | -9.9 | $CDCl_3$ | HRMS | [13] |
| | *p*-$OCH_3$ | -8.6 | $CDCl_3$ | FTIR; MS | [4] |
| | *m*-$OCH_3$ | -11.1 | $CDCl_3$ | MS | [13] |
| | *p*-Cl | -10.0 | $CDCl_3$ | FTIR; MS | [4] |
| | *m*-Cl | -12.6 | $CDCl_3$ | FTIR; MS | [4] |
| | *m*-$CF_3$ | -11.2 | $CDCl_3$ | FTIR; MS | [4] |
| | *m*-$CF_3$ | -12.8 | $CDCl_3$ | MS | [13] |
| | *p*-$CF_3$ | -10.5 | $CDCl_3$ | FTIR; MS | [4] |
| | *p*-F | -10.7 | $CDCl_3$ | MS | [13] |
| | *m*-F | -12.5 | $CDCl_3$ | MS | [13] |
| | *p*-Cl | -11.5 | $CDCl_3$ | Melting point | [3] |
| | *p*-Br | -11.9 | $CDCl_3$ | Melting point | [3] |
| | *m*-CN | -11.7 | $CDCl_3$ | FTIR; MS | [4] |
| | *p*-CN | -9.5 | $CDCl_3$ | FTIR; MS | [4] |
| | -H | -10.2 | $CDCl_3$ | FTIR; MS | [4] |
| | *p*-$CH_3$ | -10.5 | $CDCl_3$ | MS | [13] |
| | *p*-$CH_3$ | -10.6 | $CDCl_3$ | Melting point | [3] |
| | *o*-$CH_3$ | -9.3 | $CDCl_3$ | Elemental Analysis | [3] |
| Triphenyl phosphate esters | -H | -19.6 | $CDCl_3$ | Melting point; FTIR | [14] |
| | *p*-$OCH_3$ | -15.3 | $CDCl_3$ | - | [15] |
| | *p*-$CH_3$ | -16.3 | $CDCl_3$ | - | [15] |
| | *p*-$CH_3$ | -19.0 | $CDCl_3$ | Melting point; FTIR | [14] |
| | *o*-$CH_3$ | -16.9 | $CDCl_3$ | - | [15] |
| | *p*-$^{t}$Bu | -16.9 | $CDCl_3$ | - | [15] |
| | *o*-$^{i}$Pr | -18.0 | $CDCl_3$ | - | [15] |
| | *p*-F | -16.7 | $CDCl_3$ | - | [15] |

| | | | | |
|---|---|---|---|---|
| *p*-Cl | -17.6 | $CDCl_3$ | - | [15] |
| *p*-Cl | -19.9 | $CDCl_3$ | Melting point; FTIR | [14] |
| *m*-Cl | -17.8 | $CDCl_3$ | - | [15] |
| *p*-I | -18.1 | $CDCl_3$ | - | [15] |
| *p*-Br | -18.1 | $CDCl_3$ | - | [15] |
| *p*-$NO_2$ | -21.8 | $CDCl_3$ | - | [15] |
| *p*-$NO_2$ | -21.8 | $CDCl_3$ | - | [14] |
| *p*-$CF_3$ | -18.7 | $CDCl_3$ | - | [15] |

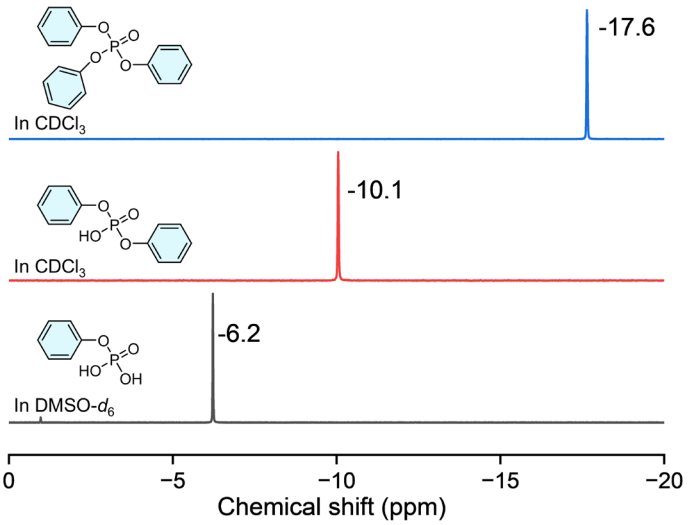


**Fig. S8.** $^{31}$P NMR spectra of commercially available monophenyl phosphate, DPP, and triphenyl phosphate.

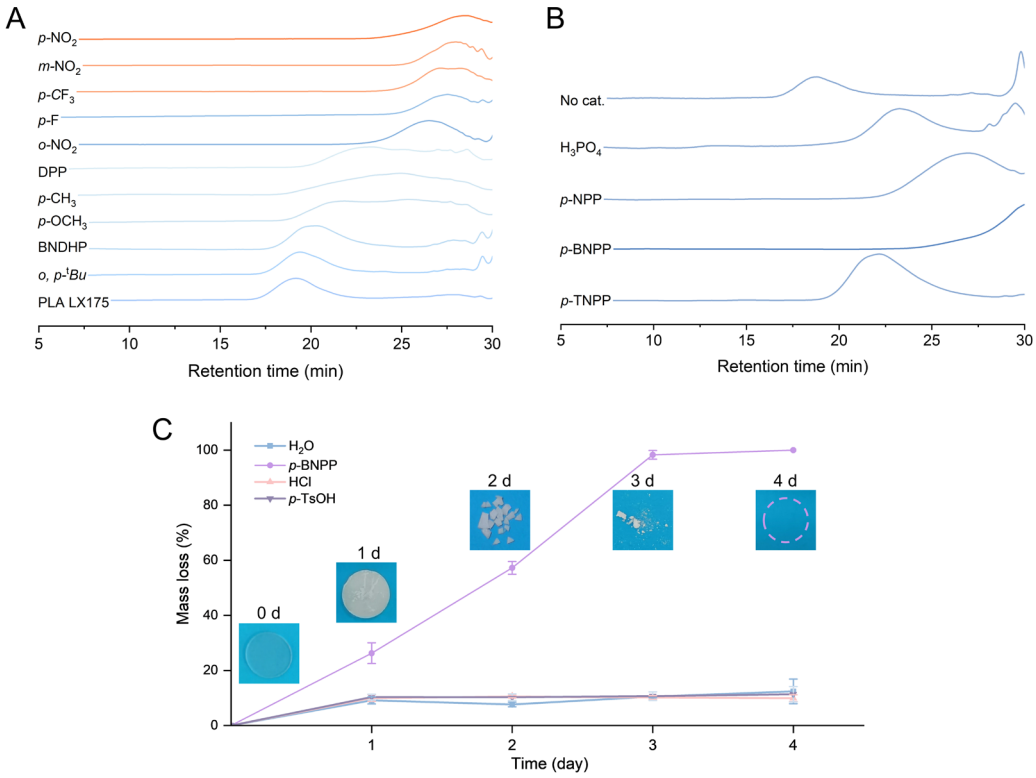


**Fig. S9.** Catalytic performances of different catalysts in the hydrolysis of PLA. GPC traces of residues after degradation of PLA catalyzed by various DPP derivatives (A) and phosphate esters (B). For DPP derivatives, reaction conditions: 1.5 g LX175 PLA, *m*(PLA): *m*(catalyst): *m*($H_2O$) = 1: 0.035: 0.3, 160 °C, 30 min. For phosphate esters, reaction conditions: 1.0 g LX175 PLA, *n*(PLA): *n*(catalyst) = 1: 0.0074, 0.3 g $H_2O$, 160 °C, 30 min. (C) Mass loss of PLA discs over time in different environments with the same pH (0.95) at 70 °C (*n* = 3), and optical photographs of collected PLA residues at indicated time points after treatment with an aqueous *p*-BNPP solution. To prevent significant pH fluctuations, the experiment was conducted at 70 °C. The dashed line indicates that there is no solid residue.

**Table S2.** MW information of PLA before and after degradation catalyzed by different DPP derivatives.

| Sample | Raw material[a)] | | Degradation product[b)] | |
|---|---|---|---|---|
| | $M_n$ (g/mol) | $Đ_M$ | $M_n$ (g/mol) | $Đ_M$ |
| *o, p*-$^t$Bu | 114,800 | 1.67 | 103,900 | 1.51 |
| -$C_4H_4$ | | | 69,600 | 1.52 |
| *p*-$OCH_3$ | | | 2,900 | 7.98 |
| *p*-$CH_3$ | | | 2,500 | 7.68 |
| DPP | | | 2,300 | 5.83 |
| *o*-$NO_2$ | | | 1,400 | 2.04 |
| *p*-F | | | 900 | 1.49 |
| *p*-$CF_3$ | | | 750 | 1.76 |
| *m*-$NO_2$ | | | 600 | 1.60 |
| *p*-$NO_2$ | | | 500 | 1.74 |

[a)] Determined by GPC in THF using PS standards for calibration.

[b)] Conditions: 1.5 g LX175 PLA, *m*(polymer): *m*(catalyst): *m*($H_2O$) = 1: 0.035: 0.3, 160 °C, 30 min. The degradation products of PLA were detected by GPC in THF using PS standards for calibration.

**Table S3.** MW information of PLA before and after degradation catalyzed by $H_3PO_4$ and different phosphate esters.

| Catalyst | Raw material[a)] | | Degradation product[b)] | |
|---|---|---|---|---|
| | $M_n$ (g/mol) | $Đ_M$ | $M_n$ (g/mol) | $Đ_M$ |
| No catalyst | | | 102,600 | 1.51 |
| $H_3PO_4$ | | | 15,600 | 1.40 |
| *p*-NPP | 114,800 | 1.67 | 2,300 | 1.96 |
| *p*-BNPP | | | Below quantification limit | |
| *p*-TNPP | | | 22,200 | 1.84 |

[a)] Determined by GPC in THF using PS standards for calibration.

[b)] Conditions: 1.0 g LX175 PLA, *n*(PLA): *n*(catalyst) = 1: 0.0074, 0.3 g $H_2O$, 160 °C, 30 min. The degradation products of PLA were detected by GPC in THF using PS standards for calibration.

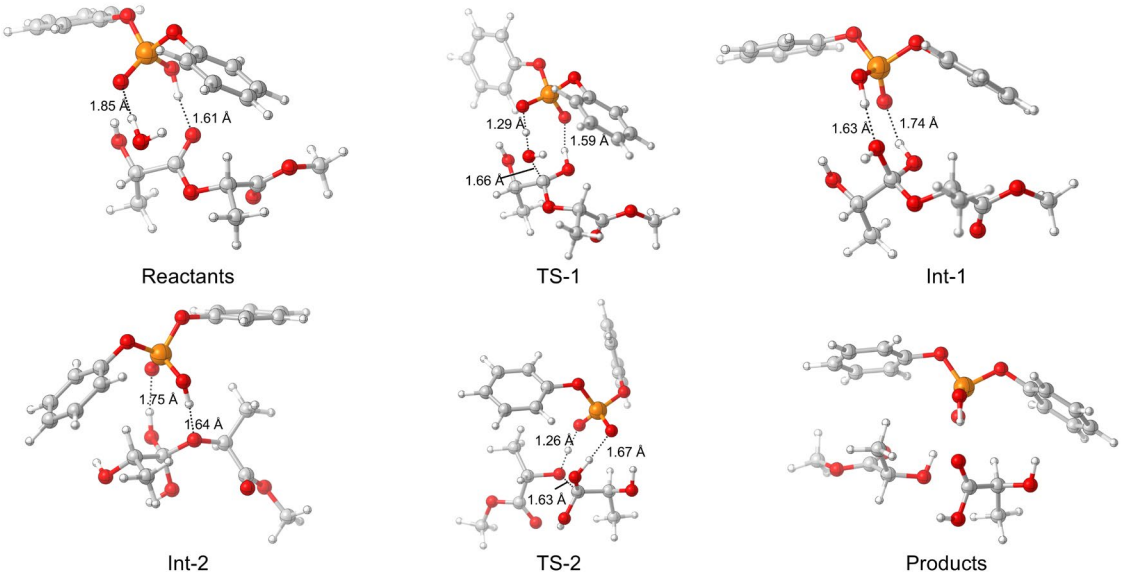


**Fig. S10.** 3D models of DPP-mediated PLA hydrolysis at different reaction stages. Color code: grey C; white H; red O; orange P.

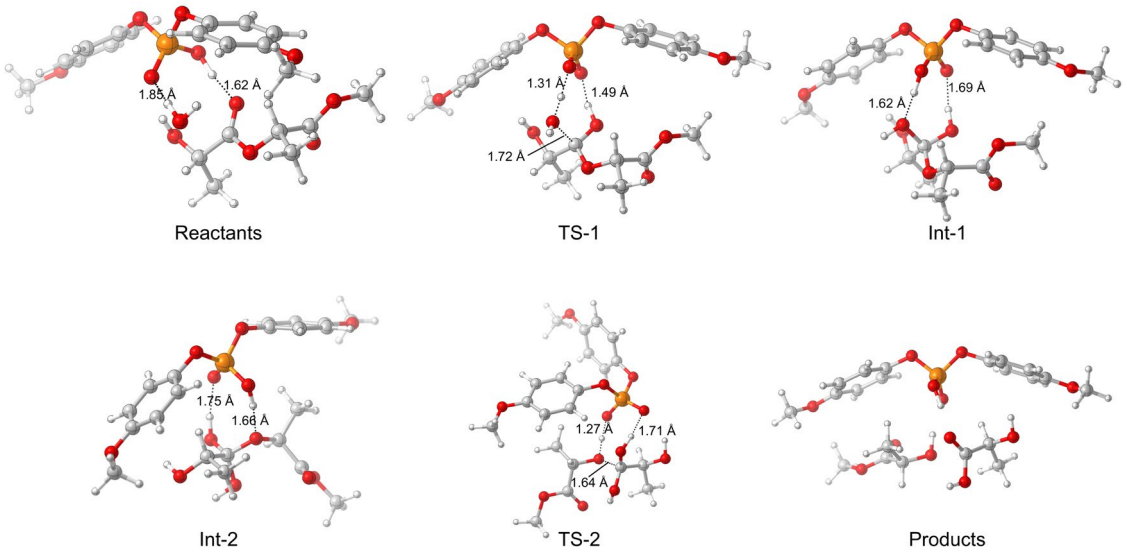


**Fig. S11.** 3D models of *p*-BMOPP-mediated PLA hydrolysis at different reaction stages. Color code: grey C; white H; red O; orange P.

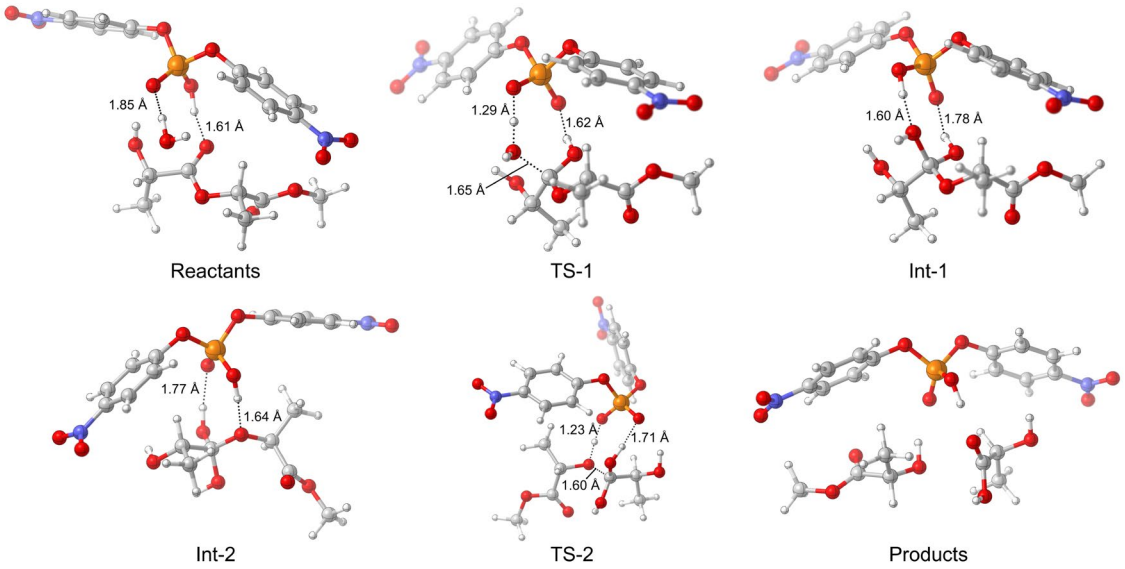


**Fig. S12.** 3D models of *p*-BNPP-mediated PLA hydrolysis at different reaction stages. Color code: grey C; white H; red O; orange P; blue N.

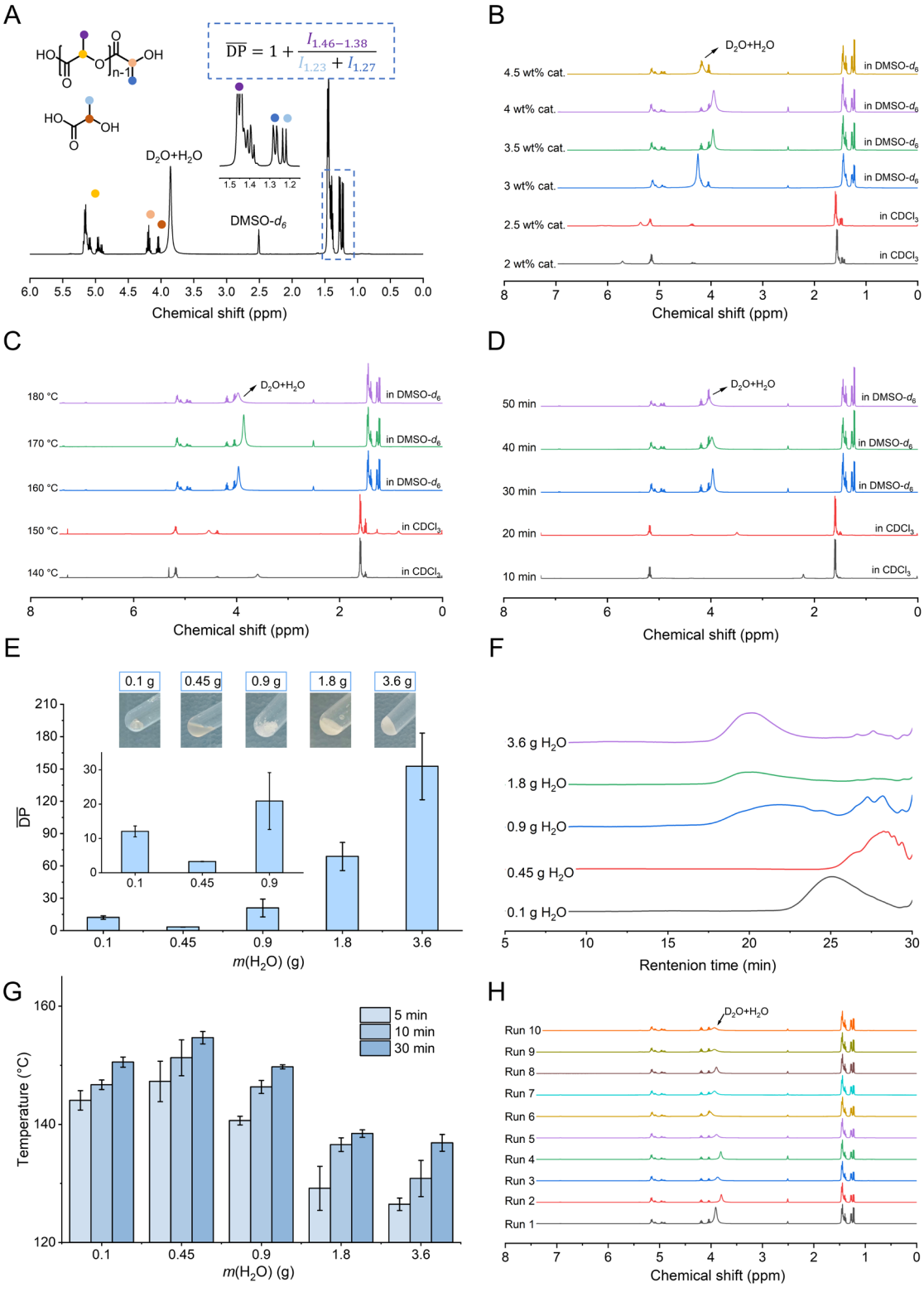


**Fig. S13.** Characterization of residues after degradation of PLA. (A) A typical $^{1}$H NMR spectrum and its peak assignments of the degradation residues. $^{1}$H NMR stacking spectra of degradation residues in different catalyst loading (B), temperature (C), reaction time (D). (E) The $\overline{DP}$ results and optical images of degradation residues in different water loading. For each group, $n$ = 3. (F) GPC traces of degradation residues in different water loading. The measurements were conducted in THF. (G) Internal temperatures of the system measured in different water loading at 5 min, 10min, and 30 min. (B-G) Typical reaction conditions: 1.5 g LX175 PLA, $m$(PLA): $m$(*p*-BNPP): $m$($H_2O$) = 1: 0.035: 0.3, 160 °C, 30 min. For each group, $n$ = 3. (H) $^{1}$H NMR stacking spectra of residues in the repeated feeding experiment from Run 1 to Run 10. Reaction conditions: 1.0 g LX175 PLA, $m$(PLA): $m$(*p*-BNPP): $m$($H_2O$) = 1: 0.035: 0.3, 160 °C, 30 min. For each group, $n$ = 3.

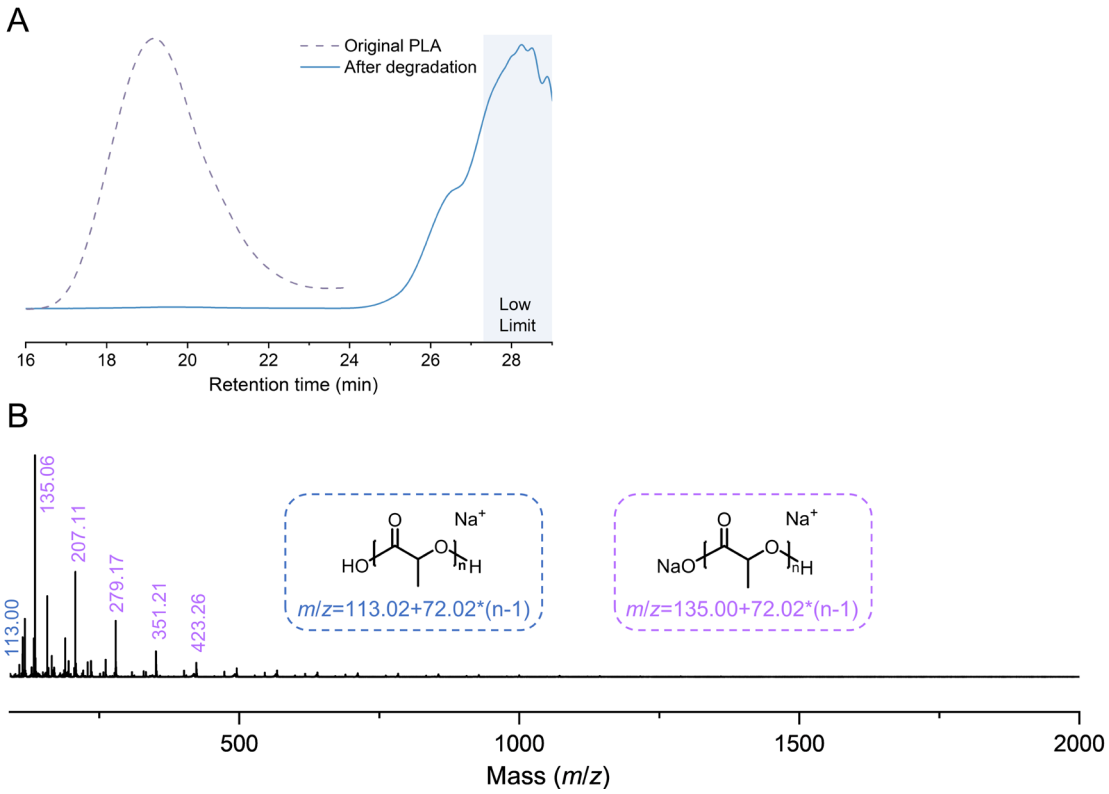


**Fig. S14.** Characterization of degradation residues obtained under optimal reaction conditions. (A) Typical GPC traces of LX175 PLA and its degradation residues. The measurements were conducted in THF. (B) MALDI-TOF mass spectrum of degradation residues.

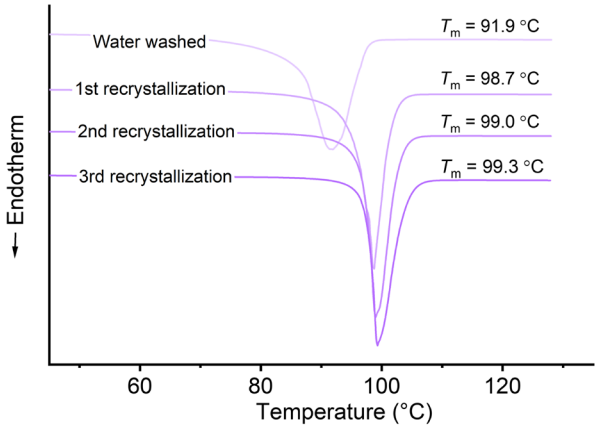


**Fig. S15.** DSC curves of LA obtained via Route A.

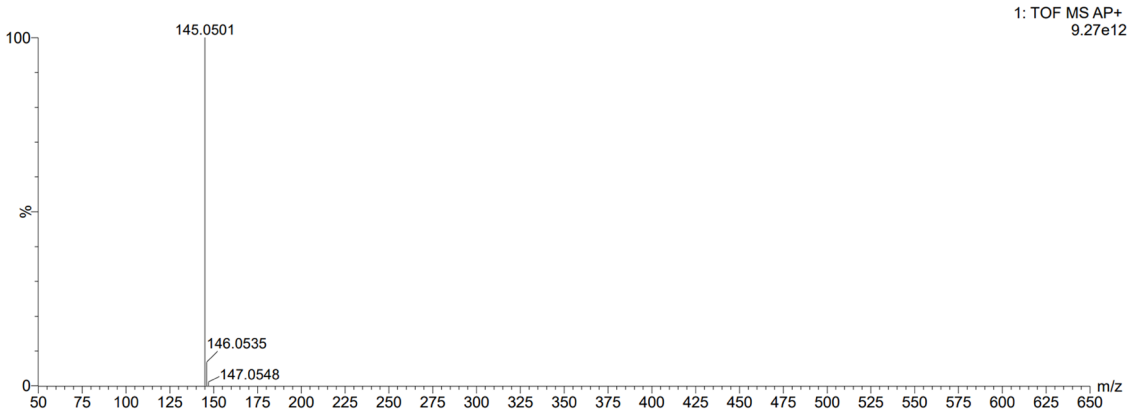


**Fig. S16.** HRMS spectrum of purified LA.

**Table S4.** Properties of original PLA and repolymerized PLA.

| Sample | $M_n$[b] (g/mol) | $Đ_M$[b] | $T_g$ (°C) | $T_{cc}$ (°C) | $T_m$ (°C) |
|---|---|---|---|---|---|
| Original PLA[a] | 133,700 | 1.64 | 59.5 | 118.4 | 152.3 |
| Repolymerized PLA | 282,900 | 1.49 | 60.9 | 109.3 | 181.7 |

[a] Luminy® LX175, TotalEnergies Corbion.

[b] Determined by GPC in $CHCl_3$ using PS standards for calibration.

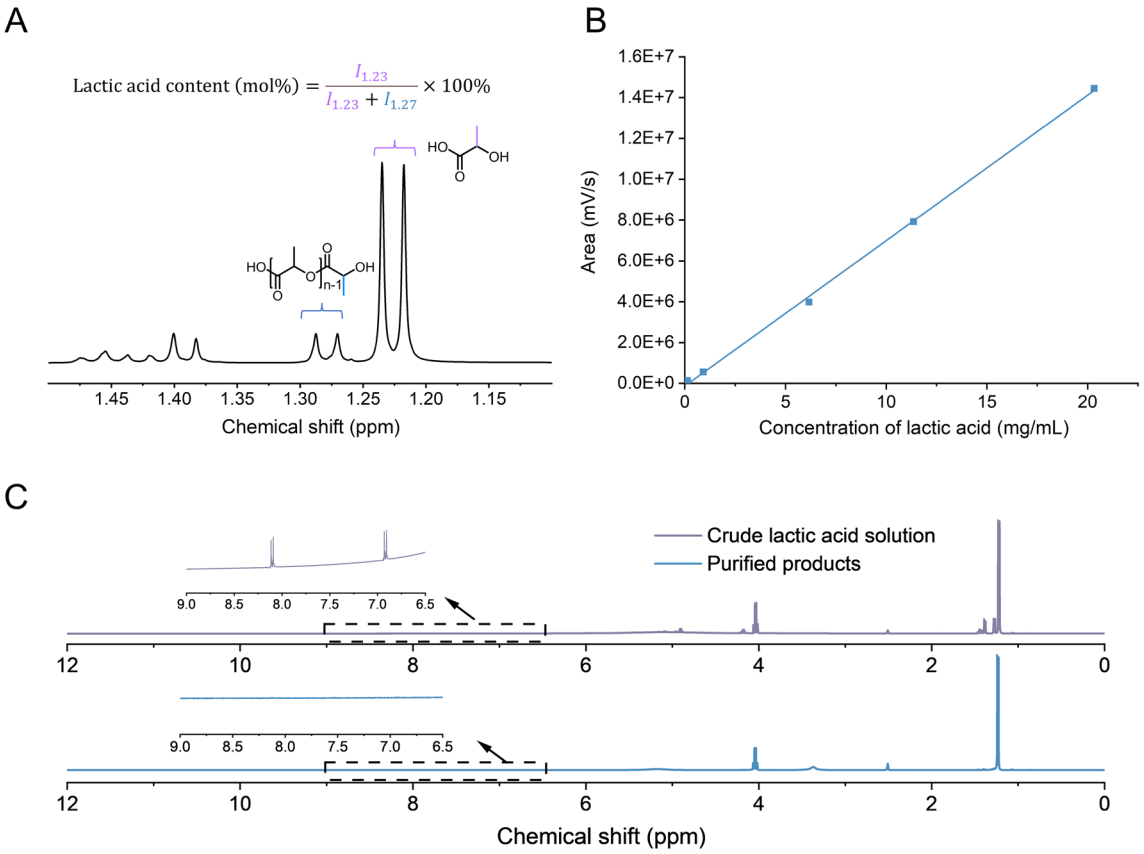


**Fig. S17.** Characterization of lactic acid solution obtained via route B. (A) A typical $^{1}$H NMR spectrum of lactic acid solution obtained from OLA. (B) Standard curve of lactic acid established by pharmaceutical-grade lactic acid. (C) $^{1}$H-NMR spectra of lactic acid solution before and after vacuum distillation.

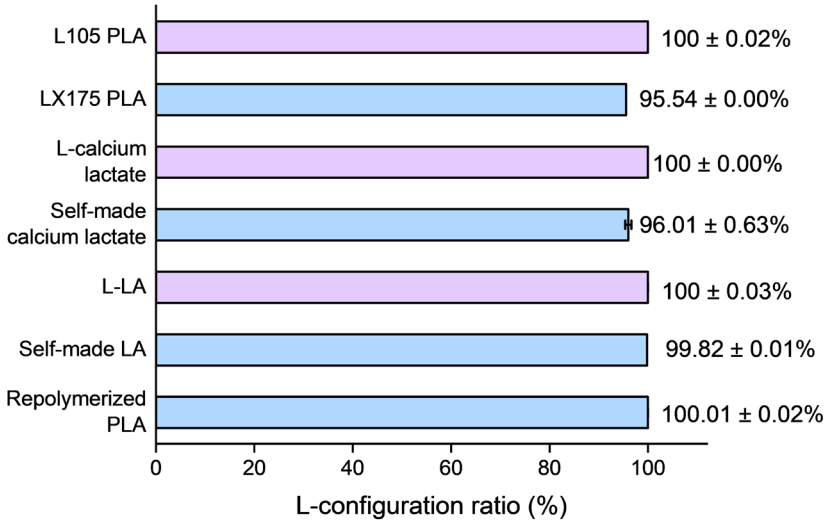


**Fig. S18.** L-configuration ratios of various samples. Self-made calcium lactate and L-calcium lactate were synthesized using lactic acid solution obtained from LX175 PLA pellets and commercial L-lactic acid, respectively. Self-made LA and repolymerized PLA were derived from the closed-loop recycling of LX175 PLA pellets. L105 PLA, LX175 PLA, and L-LA are commercial products. For each group, $n$ = 3.

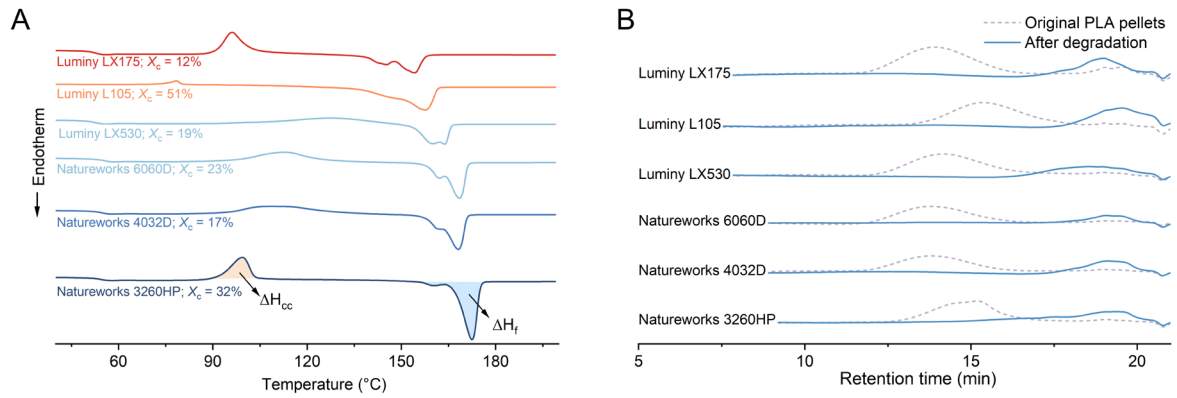


**Fig. S19.** Properties of original PLA pellets and their degradation residues. (A) DSC traces of original PLA pellets and their $X_c$ data. (B) GPC traces of original PLA pellets and their degradation residues. The measurements were conducted in $CHCl_3$.

**Table S5.** MW information of different PLA pellets before and after degradation.

| Sample | Raw material[a)] | | Degradation product[b)] | |
|---|---|---|---|---|
| | $M_n$ (g/mol) | $Đ_M$ | $M_n$ (g/mol) | $Đ_M$ |
| Luminy® LX175, TotalEnergies Corbion | 133,700 | 1.64 | Below quantification limit | |
| Luminy® L105, TotalEnergies Corbion | 38,800 | 1.88 | | |
| Luminy® LX530, TotalEnergies Corbion | 111,900 | 1.63 | | |
| Ingeo™ 6060D Natureworks | 147,300 | 1.62 | | |
| Ingeo™ 4032D Natureworks | 151,000 | 1.55 | | |
| Ingeo™ 3260HP Natureworks | 76,000 | 1.56 | | |

[a)] Determined by GPC in $CHCl_3$ using PS standards for calibration.

[b)] Conditions: 1.5 g PLA, *m*(PLA): *m*(*p*-BNPP): *m*($H_2O$) = 1: 0.035: 0.3, 160 °C, 30 min. The degradation products of PLA were detected by GPC in $CHCl_3$ using PS standards for calibration.

**Table S6.** MW information of different polyester/polycarbonate plastics before and after degradation.

| Sample | Raw material[a] | | Degradation product[b] | |
|---|---|---|---|---|
| | $M_n$ (g/mol) | $Đ_M$ | $M_n$ (g/mol) | $Đ_M$ |
| PBAT | 12,900 | 1.78 | 600 | 1.68 |
| PBS | 32,400 | 1.69 | 600 | 1.62 |
| PCL | 44,400 | 1.40 | 1,000 | 1.98 |
| PTMC | 95,500 | 1.62 | 800 | 4.30 |
| PBSA | 79,000 | 1.68 | 1,000 | 1.60 |
| PHB | 327,600 | 1.69 | 600 | 3.15 |

[a] Determined by GPC in THF (for PBAT, PBS, PCL, PTMC) or $CHCl_3$ (for PBSA, PHB) using PS standards for calibration.

[b] Conditions: 1.5 g polymer, *m*(polymer): *m*(*p*-BNPP): *m*($H_2O$) = 1: 0.035: 0.3, 160 °C, 30 min. For PHB, the reaction time was prolonged to 2 h. The degradation products of polyester/polycarbonate plastics were detected by GPC in THF (for PBAT, PBS, PCL, PTMC) or $CHCl_3$ (for PBSA, PHB) using PS standards for calibration.

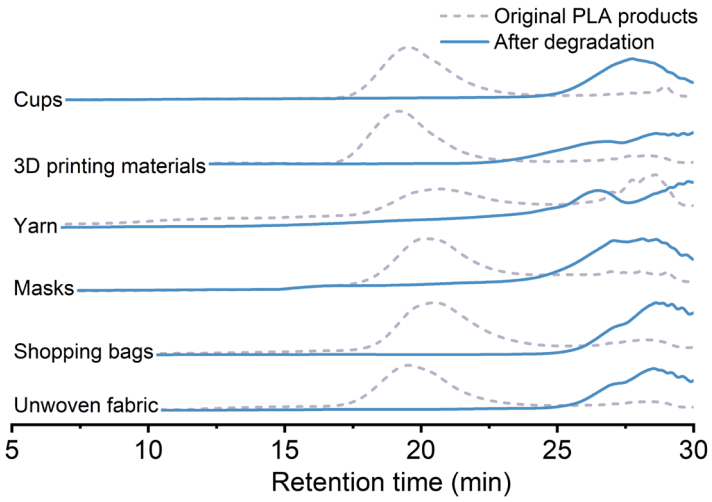


**Fig. S20.** GPC traces of original PLA products and their degradation residues. The measurements were conducted in THF.

**Table S7.** MW information of different PLA products before and after degradation.

| PLA products | Raw material[a)] | | Degradation product[b)] | |
|---|---|---|---|---|
| | $M_n$ (g/mol) | $Đ_M$ | $M_n$ (g/mol) | $Đ_M$ |
| Cups | 89,500 | 1.60 | 800 | 1.51 |
| 3D printing materials | 125,800 | 1.53 | 1,000 | 2.25 |
| Yarn | 48,900 | 1.77 | 1400 | 1.47 |
| Masks | 67,800 | 1.54 | 700 | 1.76 |
| Shopping bags | 52,300 | 1.63 | 500 | 1.39 |
| Unwoven fabric | 86,500 | 1.61 | 600 | 1.50 |

[a)] Determined by GPC in THF using PS standards for calibration.

[b)] Conditions: 1.5 g PLA products, *m*(PLA products): *m*(*p*-BNPP): *m*($H_2O$) = 1: 0.035: 0.3, 160 °C, 30 min. The degradation products of PLA were detected by GPC in THF using PS standards for calibration.

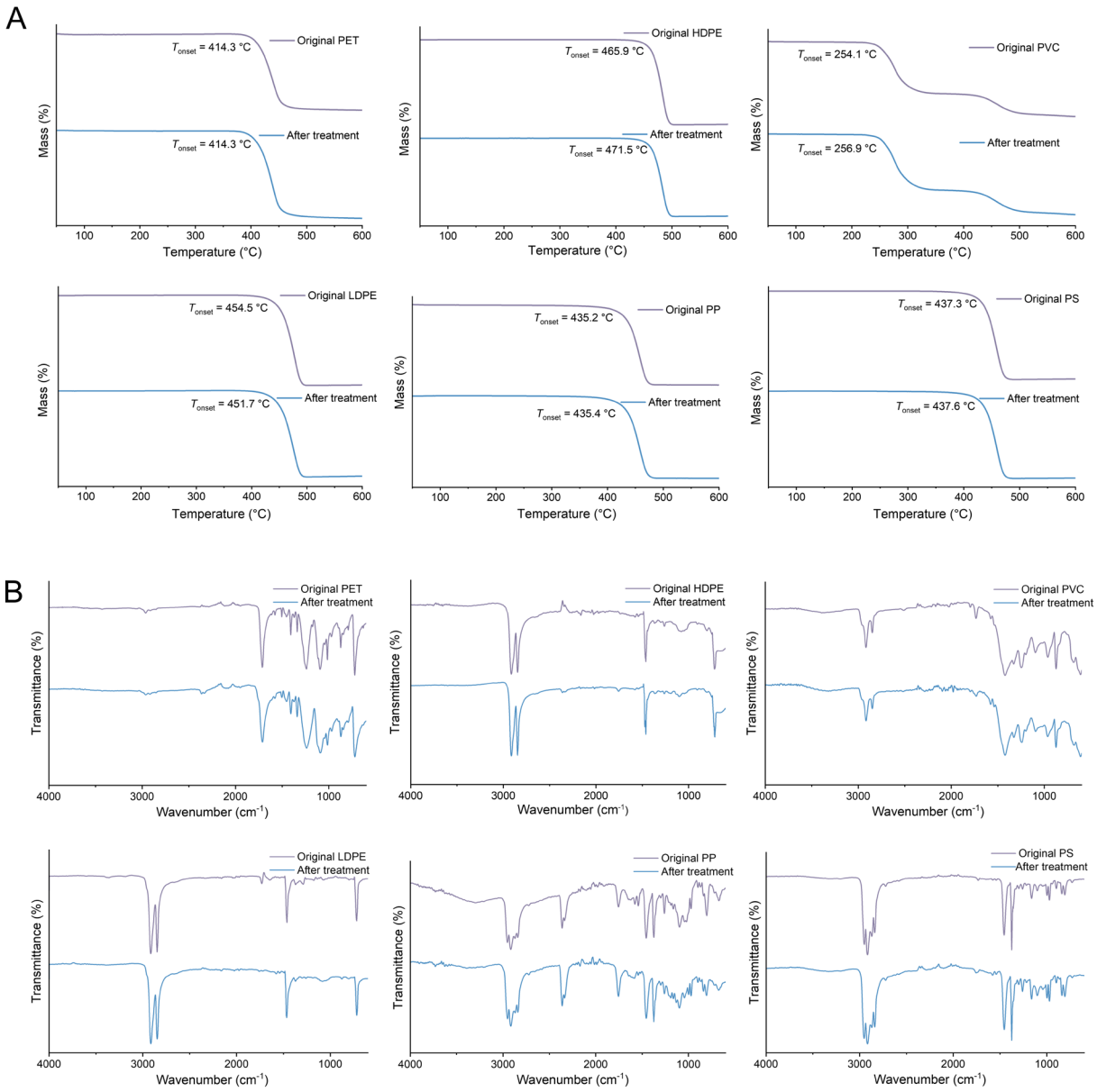


**Fig. S21.** Properties of durable plastics before and after treatment in the presence of *p*-BNPP. (A) TGA thermograms of PET, HDPE, PVC, LDPE, PP and PS before and after treatment. (B) ATR-FTIR spectra of PET, HDPE, PVC, LDPE, PP and PS before and after treatment.

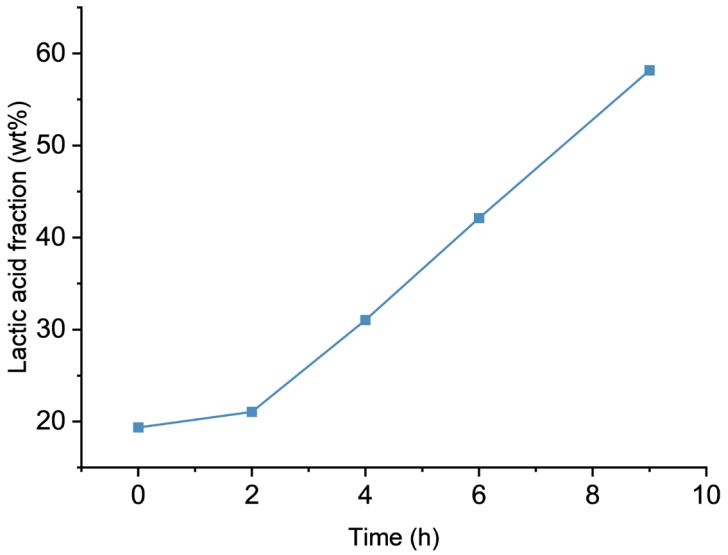


**Fig. S22.** Changes in mass fraction of lactic acid over reaction time.

**Table S8.** Comparison of the catalytic performances of *p*-BNPP with the previously reported catalysts for PLA hydrolysis.

| Catalyst | Mass ratio of solvent/PLA | Mass ratio of catalyst/PLA | Temperature (°C) | Time (min) | Yield (%) | Product | $\varepsilon$ ($°C^{-1}·min^{-1}$) | *E* factor (a.u.) | $\xi$ factor (°C·min) | Ref. |
|---|---|---|---|---|---|---|---|---|---|---|
| *p*-BNPP | 0.3 | 0.035 | 160 | 30 | 92 | OLA (250 g/mol) | 1.92E-4 | 0.066 | 3.43E+2 | This work |
| DPP | 0.3 | 0.035 | 160 | 90 | 92* | OLA (200 g/mol) | 6.39E-5 | 0.065 | 1.02E+3 | [16] |
| No cat. | 20 | 0 | 180 | 120 | 95 | Lactic acid | 4.40E-5 | 1.684 | 3.83E+4 | [17] |
| *Proteinase K* | 125.025 | 0.025 | 37 | 4680 | 76 | Lactic acid | 4.39E-6 | 13.187 | 3.00E+6 | [18] |
| MK 10 | 8.72 | 4 | 100 | 360 | 93 | OLA (300 g/mol) | 2.58E-5 | 4.926 | 1.91E+5 | [19] |
| MK 5 | 10.464 | 4 | 100 | 60 | 90 | OLA (300 g/mol) | 1.50E-4 | 5.273 | 3.52E+4 | [20] |
| HiC | 4.5 | 0.0065 | 55 | 5760 | 65 | Lactic acid | 2.05E-6 | 0.562 | 2.74E+5 | [21] |
| ZnO-ZrO | 500 | 2.6 | 130 | 4320 | 99 | Lactic acid | 1.76E-6 | 42.505 | 2.42E+7 | [22] |
| $H_2SO_4$ | 1 | | 160 | 90 | 92 | Lactic acid | 6.39E-5 | 0.087 | 1.36E+3 | [23] |
| [Bmim][OAc] | 2 | 0.5 | 130 | 120 | 83 | Lactic acid | 5.32E-5 | 0.675 | 1.27E+4 | [24] |
| HTMAB | 8 | 0.1 | 100 | 10.2 | 90 | Lactic acid | 8.82E-4 | 0.800 | 9.07E+2 | [25] |
| 2-HEAA | 6 | 2.5 | 140 | 180 | 72 | Lactic acid | 2.86E-5 | 3.444 | 1.20E+5 | [26] |
| NaOH | 33.3 | | 160 | 60 | 100 | Lactic acid | 1.04E-4 | 2.664 | 2.56E+4 | [27] |
| $ZnL_2(NO_3)_2$ | 31.25 | 0.00625 | 60 | 1080 | 70 | Lactic acid | 1.08E-5 | 3.579 | 3.31E+5 | [28] |

* The result is obtained by repeating the experiment.

## 4. Supplementary References


1. E. W. Fischer, H. J. Sterzel and G. Wegner, *Kolloid Z. Z. Polym.* , 1973, **251**, 980-990.
2. E. Barnard, J. J. Rubio Arias and W. Thielemans, *Green Chem.*, 2021, **23**, 3765-3789.
3. I. E. Nifant'ev, A. N. Tavtorkin, S. y. A. Korchagina, I. F. Gavrilenko, N. N. Glebova, N. N. Kostitsyna, V. A. Yakovlev, G. N. Bondarenko and M. P. Filatova, *Appl. Catal. A: Gen.*, 2014, **478**, 219-227.
4. E. K. Macdonald and M. P. Shaver, *Eur. Polym. J.*, 2017, **95**, 702-710.
5. A. J. Kirby, M. Medeiros, P. S. Oliveira, E. S. Orth, T. A. Brandão, E. H. Wanderlind, A. Amer, N. H. Williams and F. Nome, *Chem. Eur. J.*, 2011, **17**, 14996-15004.
6. J. G. Moffatt and H. G. Khorana, *J. Am. Chem. Soc.*, 1957, **79**, 3741-3746.
7. C. Hansch, A. Leo and R. J. C. r. Taft, *Chem. Rev.*, 1991, **91**, 165-195.
8. M. J. Frisch, G. W. Trucks, H. B. Schlegel, G. E. Scuseria, M. A. Robb, J. R. Cheeseman, G. Scalmani, V. Barone, G. A. Petersson, H. Nakatsuji, X. Li, M. Caricato, A. Marenich, J. Bloino, B. G. Janesko, R. Gomperts, B. Mennucci, H. P. Hratchian, J. V. Ortiz, A. F. Izmaylov, J. L. Sonnenberg, D. Williams-Young, F. Ding, F. Lipparini, F. Egidi, J. Goings, B. Peng, A. Petrone, T. Henderson, D. Ranasinghe, V. G. Zakrzewski, J. Gao, N. Rega, G. Zheng, W. Liang, M. Hada, M. Ehara, K. Toyota, R. Fukuda, J. Hasegawa, M. Ishida, T. Nakajima, Y. Honda, O. Kitao, H. Nakai, T. Vreven, K. Throssell, J. A. Montgomery, Jr., J. E. Peralta, F. Ogliaro, M. Bearpark, J. J. Heyd, E. Brothers, K. N. Kudin, V. N. Staroverov, T. Keith, R. Kobayashi, J. Normand, K. Raghavachari, A. Rendell, J. C. Burant, S. S. Iyengar, J. Tomasi, M. Cossi, J. M. Millam, M. Klene, C. Adamo, R. Cammi, J. W. Ochterski, R. L. Martin, K. Morokuma, O. Farkas, J. B. Foresman, and D. J. Fox, Gaussian 09, Revision D.01, 2016.
9. S. Grimme, J. Antony, S. Ehrlich and H. Krieg, *J. Chem. Phys.*, 2010, **132**, 154104.
10. C. Y. Legault, CYLview, 1.0 b, 2009.
11. M. L. Nielsen, J. V. Pustinger and J. Strobel, *J. Chem. Eng. Data.*, 1964, **9**, 167-170.
12. Q. Han, L. Zhang, C. He, J. Niu and C. Duan, *Inorg. Chem.*, 2012, **51**, 5118-5127.
13. C. C. Tran, K. Asao, T. Sasaki, Y. Hayakawa and S.-i. Kawaguchi, *Tetrahedron Lett.*, 2022, **96**, 153726.
14. G. Ilia, S. Iliescu and A. Popa, *Green Chem.*, 2005, **7**, 217-218.
15. X. Huang, X. Zhao, M. Zhang, Y. Xu, H. Zhi and J. Yang, *ChemistrySelect*, 2017, **2**, 11007-11011.
16. W. Wu, H. Zhai, K. Wu, X. Wang, W. Rao, J. Ding and L. Yu, *Chem. Eng. J.*, 2024, **480**, 148131.
17. H. Tsuji, T. Saeki, T. Tsukegi, H. Daimon and K. Fujie, *Polym. Degrad. Stab.*, 2008, **93**, 1956-1963.
18. S. Li and S. McCarthy, *Macromolecules*, 1999, **32**, 4454-4456.
19. K. Okamoto, K. Toshima and S. Matsumura, *Macromol. Biosci.*, 2005, **5**, 813-820.
20. Y. Tsuneizumi, M. Kuwahara, K. Okamoto and S. Matsumura, *Polym. Degrad. Stab.*, 2010, **95**, 1387-1393.
21. M. Pérez-Venegas, T. Friščić and K. Auclair, *ACS Sustain. Chem. Eng.*, 2023, **11**, 9924-9931.
22. F. Liguori, W. Oberhauser, E. Berretti, L. Poggini, P. Barbaro and C. Moreno-Marrodán, *Adv. Energy Sustain. Res.*, 2025, **6**, 2400349.
23. D. Chauliac, P. C. Pullammanappallil, L. O. Ingram and K. T. Shanmugam, *J. Polym. Environ.*, 2020, **28**, 1503-1512.
24. X. Song, H. Wang, X. Yang, F. Liu, S. Yu and S. Liu, *Polym. Degrad. Stab.*, 2014, **110**, 65-70.
25. M. N. Siddiqui, L. Kolokotsiou, E. Vouvoudi, H. H. Redhwi, A. A. Al-Arfaj and D. S. Achilias, *J. Polym. Environ.*, 2020, **28**, 1664-1672.
26. A. Cháfer, O. Gil-Castell, A. Björling, R. Ballesteros-Garrido, J. P. Cerisuelo-Ferriols and J. D. Badia, *Resour. Conserv. Recycl.*, 2024, **210**, 107826.
27. M. Yagihashi and T. Funazukuri, *Ind. Eng. Chem. Res.*, 2010, **49**, 1247-1251.
28. S. Zhang, Q. Hu, Y.-X. Zhang, H. Guo, Y. Wu, M. Sun, X. Zhu, J. Zhang, S. Gong, P. Liu and Z. Niu, *Nat. Sustain.*, 2023, **6**, 965-973.